ELSEVIER

Palaeogeography, Palaeoclimatology, Palaeoecology 313 (1997) 183–205

PALAEO

Faunal and geochemical evidence for changes in intermediate water temperature and salinity in the western Coral Sea (northeast Australia) during the Late Quaternary

Thierry Corrège [a,b,*], Patrick De Deckker [b]

[a] *ORSTOM, Laboratoire des Formations Superficielles, 32 Avenue Varagnat, F-93143 Bondy, Cedex, France*
[b] *Department of Geology, Australian National University, Canberra, ACT 0200, Australia*

Received 15 May 1995; accepted 23 August 1996

Abstract

Ostracod assemblages and geochemical analyses of valves of specific ostracod taxa are used to reconstruct, both qualitatively and quantitatively, bottom-water temperatures (BWT) for the last 100,000 years in the western Coral Sea. The investigated core (51GC21) is situated in the lower reaches of the Antarctic Intermediate Water, at 1630 m water depth. First, we ran a Principal Coordinate Analysis (PCoA) of 42 surface samples from the Coral Sea, and then compared fossil assemblages with results of the PCoA. In addition, we selected well preserved specimens of the two genera *Krithe* and *Bythocypris* for Mg/Ca analyses.

The Mg/Ca is used to infer past changes in BWT for intermediate waters of the western Coral Sea; results indicate large temperature fluctuations over the last 100,000 years. Of interest is the documentation that the BWT was similar to the present-day temperature during part of Isotope Stage 3.

Comparison between our temperature record and the benthic foraminifer $\delta^{18}O$ record of core 51GC21, and with the $\delta^{18}O$ variations in seawater, as reconstructed by Labeyrie et al. (1987), allowed assessment of past changes in BWT salinity and density. Thus, we identify for the western Coral Sea three distinct periods on the basis of water mass density changes (i.e. for Isotope Stage 1, Stages 2, 3 and 4, and Stage 5). Our temperature record also indicates a good correlation with the 60°S summer insolation calculations for the period between 25,000 yr B.P. and 75,000 yr B.P. Comparison of our results from this study with other records from the western Pacific (the Ontong Java Plateau in particular) reveal the role of New Guinea as an oceanographic barrier. A wet phase recorded on continental Australia coincides with our high bottom-water temperature record for isotopic Stage 3. © 1997 Elsevier Science B.V.

1. Introduction

One of the key problems in palaeoceanography today is the reconstruction of the changes in global oceanic circulation with time. This circulation is driven by differences in density between the various water masses and is therefore the direct result of temperature and salinity differences. One way to assess deep-sea palaeotemperatures is to use the oxygen isotopic composition of benthic foraminifers (Duplessy et al., 1970). This approach implies that the component of the $\delta^{18}O$ record due to changes in sea level can be narrowly constrained.

* Corresponding author. Fax: +33 1 48473088.
E-mail: correge@bondy.orstom.fr.

PII S0031-0182(97)00003-5

The $\delta^{18}O$ can also vary as a function of salinity (Craig and Gordon, 1965), although this factor has generally been considered to be of minor importance in previous studies (Savin, 1977). However, discrepancies exist amongst the various deep-sea temperature reconstructions for the last glacial/interglacial interval (Chappell and Shackleton, 1986; Labeyrie et al., 1987), indicating that oxygen isotopes alone cannot provide a satisfactory answer to this crucial problem. To determine past temperatures and salinities precisely, we therefore need an independent way of calculating one of these two parameters.

Here, we take both a qualitative approach and a quantitative one, involving the study of benthic ostracods (Crustacea), to assess past changes in deep-sea temperature. The first approach is based on a comparison of fossil ostracod assemblages with a data set of 42 surface sediment samples from the Coral Sea. Corrège (1993c) showed that the bathymetric distribution of modern ostracod assemblages can be related to physicochemical characteristics of the water masses and, in particular, to bottom temperature. The second approach consists in an investigation of the chemical composition of ostracod valves. Recent studies (Corrège, 1993a,b) indicate that the incorporation of Mg in the calcitic valves of benthic ostracods is controlled by temperature, and that this relationship can be quantified. Both approaches are used here to reconstruct temperature changes based on ostracods from a core (Core 51GC21), located in the western Coral Sea (southwest Pacific Ocean), which is situated today at the base of the Antarctic Intermediate Water (AAIW). The quantification of past temperatures, coupled with the oxygen isotopic record of benthic foraminifers found in association with the ostracods, enables the reconstruction of past bottom-water salinity and density.

2. Material

2.1. Collection of modern ostracods

The material was collected from a series of Smith–McIntyre grab samples retrieved during two RV *Franklin* cruises over the Coral Sea. Care was taken to ensure that the sediment/water interface remained undisturbed when the sample was brought on deck. The upper few millimetres of each sample, covering a surface area of $0.2m^2$, were collected and the material washed with fresh water through a 100 μm nylon sieve prior to preservation in 100% ethanol. Ostracod valves were separated from the sediment in the onshore laboratory under a standard micropalaeontological binocular microscope. Selected specimens were kept in ethanol after washing several times in milliQ® water. Thorough examination of individual valves was performed at high power (×360) under the binocular microscope to determine the cleanliness of the valves. Some single valves kept in ethanol in glass scintillation vials were placed for less than 1 sec at a time in an ultrasonic bath to separate adhering particles, especially those trapped under the inner lamella, from the valves.

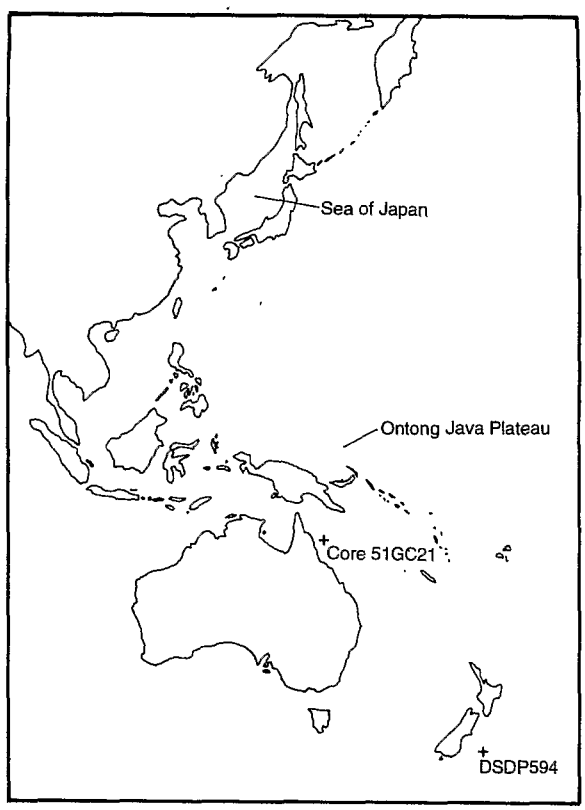

Fig. 1. Map of the southwest Pacific Ocean with major locations and cores discussed in the text.

2.2. Core 51GC21

Core 51GC21 (Latitude: 15°32.505'S; Longitude: 146°56.47'E) is located at 1630 m water depth on the western side of the Queensland Plateau (Fig. 1). It consists of an orange–brown foram sand in the upper 80 cm of the core that is separated from a grey–green foram sand below by a thin (1 cm thick), layer of grey sandy pumice. Apart from that layer, siliciclastics are rare in the upper 120 cm of the core, and only a minor amount of volcanic debris was found, at 28 cm bsf and 56 cm bsf. Beiersdorf (1989) suggested a transport by wind or as pumice rafts for these siliciclastics. A search for shallow-water ostracods in the core was also made to determine the presence of any possible up-slope contamination from the nearby Bougainville Reef. Only a few sighted ostracods (i.e. ostracods living in the 0–500 m depth interval) were encountered at 24 cm bsf and 43 cm bsf but, in both samples, the in situ fauna largely dominated the assemblage. We concluded, therefore, that Core 51GC21 represents an undisturbed record of sedimentation in its upper 120 cm.

3. Methods

3.1. Preparation of the samples and chemical analyses

Samples weighing on average 10 g were taken every 4–6 cm in the upper 120 cm of the core. Preparation of the ostracods for identification and chemical analyses are described in more detail elsewhere (Corrège, 1993a,c). This procedure involves soaking of the raw sediment samples in 3% hydrogen peroxide for a few days, then washing those samples through a 100 μm sieve and drying the residue in an oven at 40°C. Ostracod valve separation and identification, and a final cleaning stage in an ultrasonic bath for the ostracods subjected to chemical analyses were performed subsequently. Each individual ostracod valve, belonging to either *Bythocypris* or *Krithe* (the only genera for which reliable equations linking Mg/Ca to water temperature have so far been established), was then dissolved in 10 ml of ultrapure 2% HNO_3. Calcium concentrations were determined by Flame Atomic Absorption Spectrophotometry (FAAS) and magnesium concentrations by Graphite Furnace Atomic Absorption Spectrophotometry (GFAAS) at the Australian National University on a GBC 906 spectrophotometer. Three replicates were measured for each sample. Relative standard deviations are typically less than 1% for Ca and 2–5% for Mg, depending on the 'freshness' of the graphite tubes. Inter-run reproducibility for the samples was 1–2% for Ca and 5–8% for Mg.

Planktonic (*Globigerinoides ruber*) and benthic (*Cibicides wuellerstorfi*) foraminifers were prepared following standard procedures, and analysed for stable isotopes of C and O by L. Labeyrie at Gif-sur-Yvette (France). Isotopic results are expressed with reference to the PDB standard. An age model was constructed for the core, based on a graphic correlation with the standard benthic record of Martinson et al. (1987).

3.2. Statistics

Corrège (1993c) has shown that the present-day bathymetric distribution of benthic ostracods, based on a set of 42 surface samples located in the Coral Sea, can be related to the physicochemical parameters of the water in which the organisms live.

In all the fossil samples ostracod generic abundance was recorded in a semiquantitative way (Table 1) similarly to the modern samples (see Corrège, 1993c). For the 67 genera encountered in the Coral Sea, the abundance is recorded as follows:

Abundance normalised to 5 g of dry sediment
Absent (value 0 in the table)
Present (value 1 in the table): 1–5 valves
Common (value 2 in the table): 6–25 valves

No genera were represented by more than 25 specimens per 5 g of dry sediment.

To compare each fossil ostracod assemblage to the modern data set of 42 surface samples, a three-step statistical method was performed, involving a Principal Coordinates Analysis (PCoA). PCoA is a powerful method of ordination, widely used in

Table 1
Ostracod generic abundance in the 20 samples from core 51GC21

Depth	4 cm	8 cm	14 cm	19 cm	24 cm	28 cm	33 cm	38 cm	43 cm	46 cm	51 cm	56 cm	62 cm	67 cm	71 cm	76 cm	81 cm	85 cm	90 cm	95 cm
Sample number	**1**	**2**	**3**	**4**	**5**	**6**	**7**	**8**	**9**	**10**	**11**	**12**	**13**	**14**	**15**	**16**	**17**	**18**	**19**	**20**
Abyssobairdia	0	0	0	0	0	0	0	0	0	0	1	0	1	0	0	0	0	0	0	0
Abyssocypris	0	0	0	0	0	0	0	0	0	0	0	0	0	0	0	0	0	0	0	0
Abyssocythere	0	0	0	1	0	0	0	0	0	0	0	0	0	0	0	0	0	1	0	0
Ambocythere	1	0	1	0	1	0	0	0	0	0	0	0	0	0	0	0	0	0	0	0
Antarcticythere	0	0	0	0	0	0	0	0	0	0	0	0	0	0	0	0	0	0	0	0
Aratrocypris	2	2	2	1	0	0	0	2	1	1	1	0	1	0	1	0	0	0	1	1
Arcacythere	0	0	0	1	1	1	0	0	0	0	0	0	1	1	0	0	0	1	0	0
Argilloecia	2	2	2	2	2	2	2	2	2	2	2	2	2	2	1	1	2	1	2	2
Australoecia	0	0	1	0	0	0	0	1	1	1	1	0	1	1	0	0	0	0	0	0
Aversovalva	1	1	1	1	0	0	1	1	1	1	1	0	0	0	0	0	0	0	0	0
Bairdia s.l.	1	1	0	1	1	0	0	0	1	0	0	0	1	0	0	0	1	0	0	1
Bradleya	1	0	1	1	1	0	1	0	0	0	0	0	0	1	0	0	1	0	0	0
Bythoceratina	0	0	0	0	1	0	0	0	1	0	1	1	0	1	0	0	1	0	0	0
Bythocypris	1	1	1	1	1	2	2	2	2	2	2	2	2	1	2	1	1	0	0	1
Chejudocythere	0	0	0	0	0	0	0	0	1	1	1	0	0	0	0	0	0	0	0	0
Cluthia	0	0	0	0	0	0	0	0	0	0	0	0	0	0	0	0	0	0	0	0
Copytus	0	0	0	0	0	0	0	0	0	0	0	0	0	0	0	0	0	0	0	0
Cytheralison	0	0	0	0	0	0	0	0	0	0	0	0	0	0	0	0	0	0	0	0
Cytherella	0	0	0	0	0	0	0	0	0	0	0	0	0	1	0	0	0	0	0	0
Cytheropteron	2	2	2	2	2	2	2	2	2	2	2	2	2	1	2	1	2	1	1	0
Danipusella	0	0	0	0	0	0	0	0	0	0	0	0	0	0	0	0	0	0	0	0
Dutoitella	0	0	0	0	0	1	1	1	1	1	1	1	0	1	0	0	1	1	0	0
Eucythere	1	1	1	1	0	0	0	0	1	0	0	1	0	1	0	0	0	0	0	0
Eucytherura	2	2	2	2	1	1	1	1	2	0	1	2	0	0	0	0	0	0	0	0
Glyphidocythere	0	0	0	0	0	0	0	0	0	0	0	0	0	0	0	0	0	0	0	0
Hanaiceratina	0	0	0	0	0	0	0	0	0	0	0	0	0	0	0	0	0	0	0	0
Hemicytherura	0	0	0	0	0	0	0	0	0	0	0	0	0	0	0	0	0	0	0	0
Henryhowella	0	0	1	0	1	2	1	0	1	1	2	2	1	1	1	1	2	0	0	0
Jonesia	0	0	0	0	0	0	0	0	0	0	0	0	0	0	0	0	0	0	0	0
Krithe	2	2	2	2	2	2	2	2	2	2	2	2	2	2	2	2	2	2	2	2
Legitimocythere	0	0	0	0	0	0	1	0	1	1	1	1	1	1	0	0	1	1	1	0
Loxocauda	0	0	0	0	0	1	0	0	0	0	0	0	0	0	0	0	0	0	0	0
Loxoconchidea	0	0	0	0	0	0	0	0	0	0	0	0	0	0	0	0	0	0	0	0
Macrocypris	0	0	0	0	0	0	0	0	0	0	0	0	1	1	0	0	0	0	0	0
Maddocksella	0	0	0	0	0	0	0	1	0	0	0	0	0	0	0	0	0	0	0	0
Microcythere	1	0	0	0	0	0	0	0	0	0	0	0	0	0	0	0	0	0	0	0

Microcytherura	0	0	0	0	0	0	0	0	0	0	0	0	0	0	0	0	0	0	0	0
Microxestoleberis	1	1	1	1	1	0	1	2	1	1	2	1	2	0	0	0	0	0	0	0
Monoceratina	0	0	1	0	0	1	0	0	0	0	0	0	0	0	0	0	0	0	0	0
Paijenborchella	0	0	1	0	1	0	0	0	0	0	0	0	0	0	0	1	0	0	0	1
Paracythere	0	0	0	0	0	0	0	0	0	0	0	0	0	0	0	0	0	0	0	0
?Paracytherois	1	2	2	1	1	0	1	1	1	1	2	2	2	0	0	1	0	0	0	0
Paradoxostoma	0	0	0	0	0	0	0	0	0	0	0	0	0	0	0	0	0	0	0	0
Parakrithe	0	0	0	0	0	0	0	0	0	0	1	0	0	0	0	0	0	0	0	0
Parakrithella	0	0	0	0	0	0	0	0	0	0	0	0	0	0	0	0	0	0	0	0
Pedicythere	2	1	2	1	2	1	0	1	1	1	2	2	1	0	0	0	0	1	0	0
Pelecocythere	1	1	1	0	1	0	1	0	1	1	0	1	1	0	1	0	1	0	1	0
Philoneptunus	0	0	0	0	0	0	0	0	0	0	0	0	0	0	0	0	0	0	0	0
Phlyctocythere	0	0	0	0	0	0	0	0	0	0	0	0	0	0	0	0	0	0	0	0
Polycope	0	1	1	0	1	0	0	0	0	1	1	0	1	0	1	0	0	0	0	0
Pontocypris	0	0	0	0	0	0	0	0	0	0	0	1	0	0	0	0	0	0	0	0
Poseidonamicus	1	0	1	0	1	1	1	2	2	2	2	1	2	1	1	1	2	1	1	1
Propontocypris	0	1	0	0	0	0	0	2	0	1	2	0	1	0	0	0	1	0	0	0
Pseudocythere	1	1	2	1	1	0	0	0	0	1	2	1	1	0	1	1	0	0	0	0
Pterygocythere	0	0	0	0	0	0	0	0	0	0	0	0	0	0	0	0	0	0	0	0
Rhombobythere	0	0	0	0	0	0	0	0	0	0	0	0	0	0	0	0	0	0	0	0
Rimacytheropteron	0	0	0	0	1	1	1	1	1	1	2	0	1	0	0	0	0	0	0	0
Ruggieriella	0	1	0	0	0	0	0	0	0	0	0	0	0	0	0	0	0	0	0	0
Rugocythereis	0	0	1	1	1	0	0	0	0	1	0	0	0	0	0	1	0	0	0	0
Saida	1	1	0	0	0	0	0	0	0	0	0	0	0	0	0	0	0	0	0	0
Sclerochilus	0	0	0	1	0	0	0	0	0	0	0	0	0	0	0	0	0	0	0	0
Semicytherura	0	1	0	0	0	0	0	0	0	0	0	0	0	0	0	0	0	0	0	0
Swainocythere	0	0	0	0	0	0	1	1	0	1	1	1	1	0	0	0	1	0	0	0
Velibythere	0	0	0	0	0	0	0	0	0	0	0	0	1	1	1	0	0	0	0	0
Xestoleberis	2	2	2	2	1	2	2	2	2	2	2	2	2	0	0	1	1	1	1	1
Xylocythere	0	0	0	0	0	0	0	0	0	0	0	0	0	0	0	0	0	0	0	0
Zabythocypris	1	1	1	0	0	0	0	0	1	0	0	0	0	1	0	0	0	0	0	0
Unidentified	**5**	**6**	**5**	**3**	**3**	**5**	**4**	**2**	**5**	**4**	**5**	**4**	**1**	**0**	**2**	**2**	**2**	**0**	**1**	**0**
Generic abundance	**25**	**26**	**28**	**21**	**25**	**19**	**21**	**20**	**28**	**27**	**30**	**23**	**25**	**17**	**13**	**13**	**17**	**10**	**9**	**8**

The depth of each sample in the core is given together with the corresponding number which appears in Fig. 6

ecological and agricultural studies (Williams, 1976; Digby and Kempton, 1987). The basis of a PCoA is a symmetric matrix that can easily be derived from a sites-by-genera matrix (Digby and Kempton, 1987). When samples treated by PCoA are ordinated along the two principal axes, a horseshoe effect is often observed. If this effect is too strong, it can obscure the results, and then alternative ordination methods have to be considered (Digby and Kempton, 1987). All the calculations were conducted with the GENSTAT package in the Department of Statistics at the Australian National University. The three-step method can be described as follows:

(1) The modern data set (see table 3 in Corrège, 1993c for raw data) was subjected to the PCoA, and the ordination is shown in Fig. 2. The samples arranged along the two principal axes of variation display a typical horseshoe pattern. While temperature is the obvious environmental factor associated with the first axis, it is more difficult to determine which factor is represented on the second axis. Dissolved oxygen is the prime candidate, but the influence of nutrients cannot be ruled out.
(2) Similarity coefficients were calculated between each fossil sample and the 42 modern surface samples.
(3) Each fossil sample was added to the PCoA without disturbing the original ordination, following the method described by Gower (1971).

The position of a fossil sample on the horseshoe

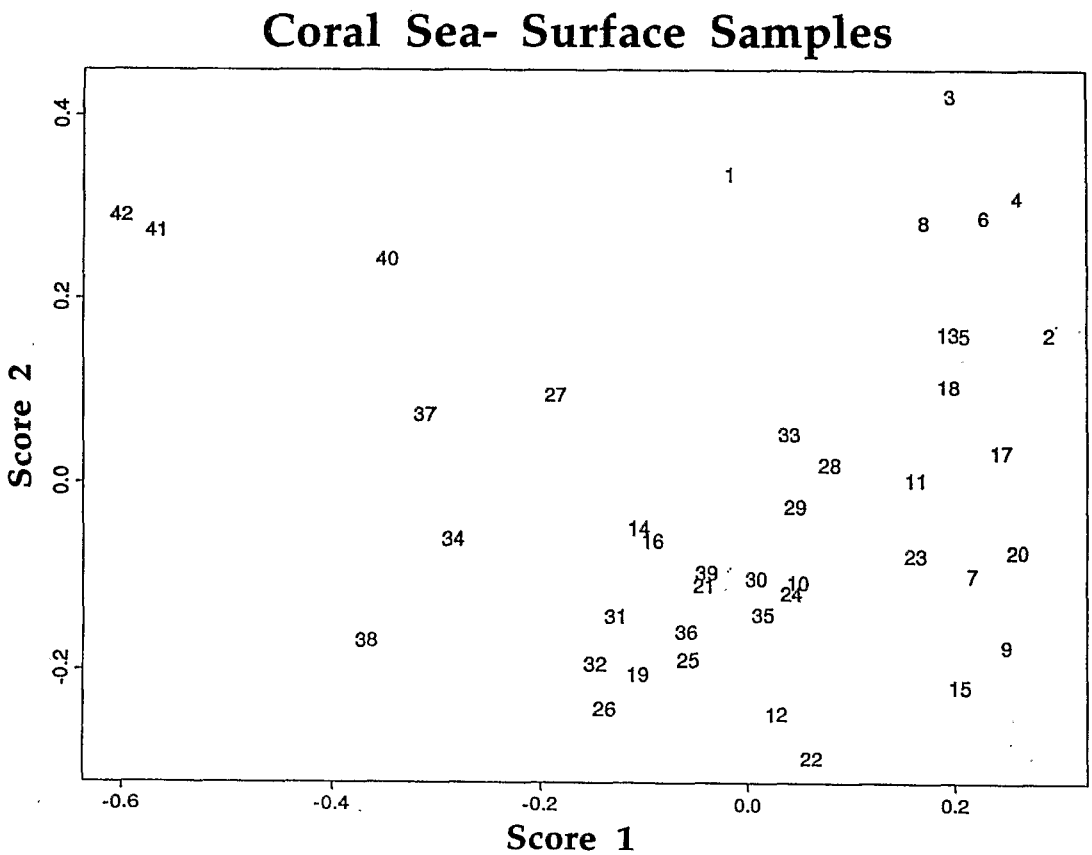

Fig. 2. Plot of Score 1 versus Score 2 for the PCoA conducted on the ostracod fauna from 42 surface samples located in the Coral Sea (see Corrège, 1993c). The numbers refer to the samples listed in table 2 in Corrège (1993c) (number 1 being the shallowest and number 42 the deepest).

pattern is, therefore, determined solely by its ostracod content and its similarity to all the modern ostracod assemblages. The movement along the horseshoe pattern of the fossil samples can then be interpreted in terms of temperature changes.

3.3. Mg/Ca versus temperature calibration

Ostracods are microscopic, bivalved crustaceans which secrete a low-Mg calcite shell through successive moulting stages (usually 8 or 9). The work of Turpen and Angell (1971) has demonstrated that, prior to moulting, there is no resorption of calcium from the shell to the soft parts of the ostracod. This indicates that the ostracod valves will be in direct equilibrium with the environment in which they are secreted. Laboratory experiments (Chivas et al., 1983, 1985, 1986a,b) on non-marine ostracods indicate a strong thermodependence for the incorporation of Mg in the calcitic shells, corroborating previous work on inorganic (Mucci, 1987; Burton and Walter, 1991) and organic (Chave, 1954; Lowenstam, 1963; Cadot, 1974; Cadot and Kaesler, 1977) calcite. Furthermore, these experiments showed that, once calcification is completed (typically within a few days), there is no additional incorporation of trace elements, such as Mg and Sr, in the valves.

The preliminary calibration equations for *Bythocypris* and *Krithe*, which have been published previously (Corrège, 1993a), have been improved by additional analyses and better statistical treatment of the data. Chemical analyses of single ostracod valves presented in Table 2 and Fig. 3 enable calculation of the relationship between water temperature in the range 2–6°C and the Mg/Ca of the ostracods:

For *Bythocypris*

$$T\ (°C) = 366 \times (\text{Mg/Ca } \textit{Bythocypris} \text{ valve}) - 6.7 \quad (1)$$

For *Krithe*

$$T\ (°C) = 520 \times (\text{Mg/Ca } \textit{Krithe} \text{ valve}) - 3.3 \quad (2)$$

We also performed a test aiming at demonstrating that the confidence level in the temperature estimation based on the above relationship for the 2 genera improves quite substantially once at least 4 ostracod valves from the same sample are analysed (Fig. 3c). A temperature reconstructed from the analyses of 4 valves has an accuracy of ± 1°C for *Bythocypris* and ± 1.35°C for *Krithe*.

Although none of the ostracods analysed were found together with soft parts (the latter would indicate that the individuals were alive at the time of collection), we are confident that the organisms selected for analysis were modern. These specimens were found together with others containing soft parts but belonging to different taxa (e.g. *Cytherella*, *Zabythocypris* and *Polycope*). Thus the samples represent biocoenoses. Additionally, several of the *Krithe* specimens had both valves still joined in the hinge area, indicating that they belonged to individuals which had died shortly before collection; it is usual for valves to separate soon after death, either due to current reworking or bacterial decay and scavenging. However, we cannot rule out some reworking, which could be an explanation for part of the scatter in the data.

It is necessary to know the Mg/Ca of the water at each locality to calculate the distribution coefficient [D = Mg/Ca ostracod valve/Mg/Ca water] for both *Bythocypris* and *Krithe*. Sea-water analyses from each collection site show a constant value for Mg/Ca of 5.2, in agreement with standard values given in the literature (Chester, 1990 and references therein). Therefore, using Eqs. (1) and (2), it is possible to calculate D for each genus:

For *Bythocypris*

$$D = 3.5 \times 10^{-3} + 5.3 \times 10^{-4} \times T \quad (3)$$

For *Krithe*

$$D = 1.2 \times 10^{-3} + 3.7 \times 10^{-4} \times T \quad (4)$$

These two equations emphasise the fact that D is dependent on temperature, and that different genera have different distribution coefficients. The finding that *Bythocypris* incorporates proportionally more Mg in its valves than *Krithe* is in agreement with previous work (Cadot, 1974; Cadot and Kaesler, 1977), and reflects the phylogenetic effect (Chave, 1954; Lowenstam, 1963) because *Bythocypris* is a more 'primitive' ostracod than *Krithe*.

It is important to ensure that only adult ostracod

Table 2
Detail of the chemical analyses for the two ostracod genera *Bythocypris* (top of table) and *Krithe* (bottom of table)

Sample	Temp	$CaCO_3$	Ca	Mg	Mg	Mg/Ca	mean Mg/Ca	Standard deviation
	(°C)	(μg)	(μg)	(μg)	(ppm)	(molar)		
29B	5.04	20.98	8.40	0.1481	7060	0.029057	0.031313	0.002518
29C	5.04	25.05	10.03	0.1798	7178	0.029541		
29D	5.04	22.00	8.81	0.1676	7621	0.031362		
29E	5.04	14.08	5.64	0.1204	8548	0.035179		
29F	5.04	22.14	8.87	0.1549	6994	0.028784		
29G	5.04	15.39	6.16	0.1283	8334	0.034299		
29H	5.04	18.84	7.55	0.1504	7981	0.032845		
29I	5.04	16.10	6.45	0.1151	7152	0.029433		
56B	4.33	33.59	13.45	0.2336	6955	0.028623	0.030540	0.002236
56C	4.33	32.33	12.95	0.2576	7968	0.032792		
56D	4.33	51.13	20.48	0.3495	6835	0.028130		
56F	4.33	27.32	10.94	0.2021	7400	0.030453		
56G	4.33	19.21	7.69	0.1601	8335	0.034301		
56H	4.33	26.80	10.73	0.1944	7254	0.029854		
56I	4.33	33.73	13.51	0.2428	7199	0.029627		
49A	3.57	41.30	16.54	0.3038	7355	0.030270	0.029067	0.002174
49B	3.57	33.06	13.24	0.2199	6652	0.027377		
49C	3.57	36.83	14.75	0.2259	6135	0.025248		
49D	3.57	20.00	8.01	0.1489	7444	0.030637		
49E	3.57	22.75	9.11	0.1588	6980	0.028725		
49G	3.57	25.78	10.32	0.1853	7186	0.029573		
49H	3.57	27.32	10.94	0.2100	7688	0.031640		
34A	2.95	29.00	11.61	0.2091	7210	0.029673	0.028048	0.001851
34B	2.95	28.73	11.51	0.1909	6643	0.027338		
34C	2.95	29.59	11.85	0.2038	6887	0.028344		
34E	2.95	32.39	12.97	0.2244	6928	0.028513		
34F	2.95	44.24	17.72	0.2608	5895	0.024260		
34G	2.95	23.86	9.56	0.1718	7197	0.029619		
34H	2.95	33.87	13.56	0.2353	6948	0.028596		
72A	2.64	61.42	24.60	0.3480	5666	0.023317	0.024404	0.003150
72B	2.64	70.30	28.15	0.3570	5078	0.020898		
72C	2.64	35.65	14.28	0.2556	7168	0.029501		
72D	2.64	43.15	17.28	0.2507	5810	0.023909		
72E	2.64	37.20	14.90	0.2205	5927	0.024394		
12A	2.29	66.08	26.46	0.3231	4889	0.020119	0.023690	0.003254
12B	2.29	63.35	25.37	0.3373	5324	0.021913		
12C	2.29	35.22	14.10	0.2181	6191	0.025479		
12D	2.29	33.53	13.43	0.2220	6621	0.027247		
107A	2.25	70.11	28.08	0.3881	5536	0.022782	0.023963	0.001860
107B	2.25	63.40	25.39	0.3718	5864	0.024135		
107C	2.25	34.44	13.79	0.1943	5641	0.023215		
107D	2.25	36.30	14.53	0.2303	6344	0.026107		
107E	2.25	28.70	11.49	0.1819	6336	0.026077		
107F	2.25	60.08	24.06	0.3133	5215	0.021464		

valves are analysed for their Mg/Ca ratio because juveniles and partially calcified ostracods grown in vitro always have a higher Mg/Ca than adults belonging to the same taxon (Chivas et al., 1983, 1986a). This indicates that Mg is incorporated initially in large concentration proportionally to calcium. Chivas et al. (1986a) noted that the Mg/Ca of large ostracod genera (e.g. the euryhaline, non-marine *Australocypris* and *Mytilocypris*, averaging 3 mm in length) have lower distribution coefficients than smaller genera (such as *Cyprideis*, with an average length of ~1 mm). This phenomenon is not surprising since small-sized ostracod genera calcify at a much higher rate that larger ones, and thus have a higher Mg/Ca and also D. Similarly, laboratory observations made on inorganic calcite (Kitano et al., 1971) indicate that several trace elements are incorporated in a non-equilibrium manner during the very early stages of crystallisation. Therefore, the temperature control on Mg uptake in ostracod shells could be indirect; temperature may affect the rate at which the ostracod precipitates its shell. D is thus not a conventional distribution coefficient according to the dictates of chemistry but is most probably dependent on the growth processes of the animal.

Table 2 (*continued*)

Sample	Temp (°C)	$CaCO_3$ (μg)	Ca (μg)	Mg (μg)	Mg (ppm)	Mg/Ca (molar)	mean Mg/Ca	Standard deviation
23KA	5.87	22.92	9.18	0.1059	4621	0.019019	0.017546	0.000986
23KB	5.87	21.58	8.64	0.0879	4075	0.016772		
23KE	5.87	22.34	8.94	0.0901	4032	0.016594		
23KF	5.87	21.07	8.44	0.0947	4492	0.018487		
23KG	5.87	19.47	7.79	0.0805	4137	0.017024		
23KH	5.87	22.21	8.89	0.0938	4223	0.017379		
29KB	5.04	26.27	10.52	0.0844	3212	0.013221	0.015848	0.001478
29KC	5.04	21.38	8.56	0.0814	3807	0.015667		
29KD	5.04	23.97	9.60	0.0856	3571	0.014695		
29KE	5.04	21.05	8.43	0.0897	4259	0.017527		
29KF	5.04	23.16	9.28	0.0880	3798	0.015629		
29KG	5.04	23.12	9.26	0.0826	3574	0.014708		
29KH	5.04	24.51	9.81	0.1043	4255	0.017513		
29KI	5.04	24.61	9.85	0.1031	4190	0.017243		
56KB	4.33	26.96	10.80	0.0714	2648	0.010898		
56KC	4.33	33.50	13.41	0.1119	3340	0.013748		
56KD	4.33	10.72	4.29	0.0441	4114	0.016931		
56KH	4.33	12.05	4.83	0.0537	4458	0.018346		
34KA	2.95	32.13	12.87	0.1002	3120	0.012839	0.013454	0.001691
34KB	2.95	41.08	16.45	0.1195	2909	0.011973		
34KD	2.95	37.34	14.95	0.1217	3258	0.013409		
34KE	2.95	29.04	11.63	0.1123	3869	0.015921		
34KF	2.95	36.84	14.75	0.1081	2933	0.012069		
34KG	2.95	33.26	13.32	0.1074	3228	0.013286		
34KH	2.95	26.56	10.63	0.0956	3600	0.014816		
34KI	2.95	32.19	12.89	0.1113	3457	0.014225		
34KJ	2.95	46.75	18.72	0.1196	2557	0.010524		
72KA	2.64	23.51	9.41	0.0611	2598	0.010690	0.012123	0.003272
72KB	2.64	30.27	12.12	0.1200	3964	0.016312		
72KC	2.64	28.20	11.29	0.0876	3106	0.012781		
72KD	2.64	31.94	12.79	0.0844	2642	0.010875		
72KF	2.64	35.98	14.41	0.0582	1617	0.006656		
72KG	2.64	26.46	10.60	0.1147	4335	0.017839		
72KH	2.64	21.42	8.58	0.0514	2397	0.009865		
72KI	2.64	29.08	11.64	0.0752	2587	0.010647		
72KJ	2.64	18.38	7.36	0.0507	2759	0.011355		
72KK	2.64	16.85	6.75	0.0582	3452	0.014206		
12KA	2.29	35.31	14.14	0.1323	3746	0.015417	0.010122	0.003255
12KB	2.29	30.56	12.24	0.0956	3127	0.012870		
12KD	2.29	27.61	11.06	0.0855	3096	0.012741		
12KF	2.29	28.83	11.54	0.0852	2954	0.012157		
12KH	2.29	29.85	11.95	0.0690	2310	0.009506		
12KI	2.29	42.70	17.10	0.1278	2992	0.012313		
12KJ	2.29	43.78	17.53	0.0903	2064	0.008493		
12KL	2.29	37.11	14.86	0.0456	1228	0.005053		
12KM	2.29	19.54	7.83	0.0495	2534	0.010430		
107KA	2.25	63.20	25.31	0.1152	1822	0.007499	0.008959	0.001383
107KB	2.25	42.07	16.85	0.0894	2124	0.008743		
107KD	2.25	38.18	15.29	0.0978	2561	0.010541		
107KE	2.25	51.11	20.47	0.0944	1846	0.007597		
107KF	2.25	47.20	18.90	0.0804	1703	0.007009		
107KG	2.25	36.53	14.63	0.0870	2382	0.009805		
107KH	2.25	20.73	8.30	0.0552	2662	0.010957		
107KJ	2.25	20.10	8.05	0.0440	2189	0.009011		

Each sample represents one ostracod valve. Mean Mg/Ca is given together with the standard deviation for each sampling site

Further work is needed to assess how other parameters such as food supply could affect the distribution coefficient. A better understanding of the factors involved in the scatter of the data (Fig. 3a,b) is crucial for the future development of this method.

Eqs. (1) and (2) are based on analyses of modern ostracod valves, which were calcified in seawater with a Mg/Ca ratio of 5.2 (i.e. the present-day value for the world ocean; see Chester, 1990). Any alteration in seawater chemistry which could change this ratio will also affect Eqs. (1)

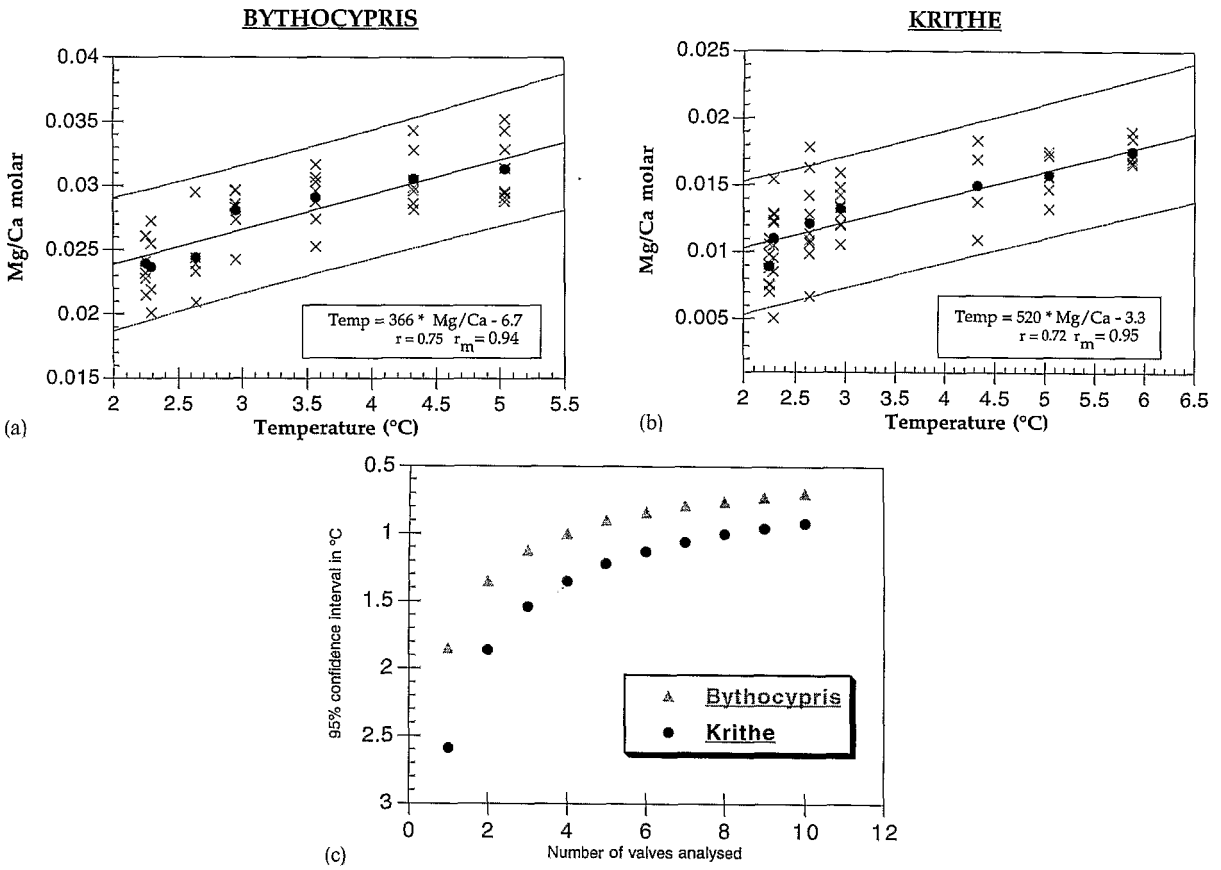

Fig. 3. (a) and (b) Plot of the Mg/Ca molar ratio of single valves (cross) versus water temperature at the collection sites in the Coral Sea offshore northeastern Australia, for the ostracods *Bythocypris* (a) and *Krithe* (b). The mean Mg/Ca for each sampling site is also plotted (dot). The regression line and the corresponding correlation coefficient value were calculated from all the data points. The correlation coefficient for the mean Mg/Ca values (r_m) is also given. (c) 95% confidence interval on a calculated palaeotemperature as a function of the number of fossil valves analysed. For example, a palaeotemperature reconstructed from the analysis of four valves will have an accuracy of ± 1°C if *Bythocypris* is used, and ± 1.35°C if *Krithe* is used.

and (2). Therefore, to use these equations for palaeotemperature estimates, we must first consider the evolution of the Mg/Ca ratio of seawater during the Late Quaternary. Since both Mg and Ca have a relatively long mean oceanic residence time (15×10^6 yr and 1.1×10^6 yr, respectively; Whitfield, 1979), this precludes any significant change in the Mg/Ca ratio of seawater for the time period considered here (the last 120,000 years). Thus, we consider that, during the last glacial/interglacial cycle, any change in the Mg/Ca ratio in ostracod valves ought to be solely controlled by temperature.

In a recent paper, Dwyer et al. (1995) successfully reconstructed bottom-water temperatures in the North Atlantic from the Mg/Ca ratio of *Krithe* valves dating back to 3.2 myr. Their method is based on ours, but they use a different calibration curve derived from analyses of core-top *Krithe* from the North Atlantic and the Arctic Ocean. The fact that the two calibrations are slightly different supports the concept that, as pointed out earlier, factors other than temperature might affect the partitioning of Mg in the ostracod valves. One of these factors may perhaps be the availability of nutrients which could affect rate of growth of the ostracods. Nutrient levels may affect the rate of calcification which, in turn, may play a role in the

uptake of some trace elements in the calcite lattice of ostracod valves. The bottom waters of the Coral Sea and the Arctic Ocean are indeed chemically dissimilar (Chester, 1990). In addition, Dwyer et al.'s (1995) calibration is based on data points covering a larger temperature span than our calibration (2–14°C for Dwyer et al. (1995), compared to 2–6°C for our present data), which could explain part of the difference in the slopes of the regression lines. We chose to use our calibration because it is based on ostracods collected in the very same area as core 51GC21. Nevertheless, it is obvious that additional work is necessary to assess whether a single calibration can be validated for all the oceans, or whether each particular oceanographic setting will need to be calibrated.

In core 51GC21 each individual fossil ostracod valve of either *Krithe* or *Bythocypris* was analysed for its Mg/Ca ratio, and the result converted to a temperature value using the relevant equation presented above. When several valves of the same genus were analysed from the same sample, a mean Mg/Ca was calculated for the whole sample, and a corresponding mean temperature subsequently inferred.

3.4. Salinity and density calculations

Palaeosalinities were calculated for each fossil level for which palaeotemperatures and benthic foraminifers $\delta^{18}O$ were available. We first added 0.83‰ to the $\delta^{18}O$ values to account for the fractionation of *C. wuellerstorfi* (Herguera et al., 1992). This step is in fact only necessary when the $\delta^{18}O$ of seawater at the studied site is known. If this information is not available, a normalisation of $\delta^{18}O$ to the Holocene value extracted from foraminifers is carried out (see below), in which case the correction for fractionation is irrelevant. Then, for each time period, we subtracted the corresponding variation in $\delta^{18}O$ of seawater compared to the present, as was reconstructed by Labeyrie et al. (1987) and Duplessy et al. (1988,)). We then normalised all the data to the surface sediment value by subtracting the $\delta^{18}O$ of the uppermost sample (i.e. 3.07‰) to the rest of the data set. This left us with a residual $\Delta T S\delta^{18}O$ which is dependant upon temperature and salinity. The reconstructed bottom palaeotemperatures (BWT) based on the Mg/Ca ratio of ostracods gave us temperature variations compared to the present-day value of 2.7°C for the site of core 51GC21. We translated these temperature variations into $\delta^{18}O$ variations assuming that a 1°C difference represents a shift of 0.23‰ in $\delta^{18}O$ terms. These $\delta^{18}O$ variations resulting from temperature are noted as $\Delta T\delta^{18}O$. We subtracted $\Delta T\delta^{18}O$ from $\Delta TS\delta^{18}O$ to obtain $\Delta S\delta^{18}O$, which is the $\delta^{18}O$ variation due to salinity. This $\Delta S\delta^{18}O$ was converted to salinity change (ΔS) assuming that a shift of 0.5‰ in $\delta^{18}O$ corresponds to a 1‰ change in salinity in the modern ocean (Craig and Gordon, 1965). However, to reconstruct palaeosalinity at a given time, t, during the last glacial period, we must take into account the increase in salinity due to the lowering of sea-level. At present, the mean ocean salinity is 34.7‰, and the average ocean water depth is 3900 m. Therefore, the difference in salinity at a given time, t, compared to the present is:

$$\Delta St = (34.7 \times LSL)/(3900 - LSL)$$

where LSL is the drop in sea-level for the period considered.

For example, a 120 m drop in sea-level (the average value for the Last Glacial Maximum) would increase the mean ocean salinity by 1.04‰ (Duplessy et al., 1991).

The palaeosalinity at a given time t can therefore be calculated as:

$$St = 34.6‰ + \Delta St + (2 \times \Delta S\delta^{18}O)$$

where 34.6‰ is the present-day salinity at site 51GC21.

Once temperature and salinity are both known for a stratigraphic horizon, the density of the water can be derived from the temperature/salinity/density diagram constructed by Labeyrie et al. (1992) and based on the equation of Cox et al. (1970).

4. Results

4.1. Stratigraphic framework

Results of the $\delta^{18}O$ analyses on benthic and planktonic foraminifers appear in Fig. 4 and

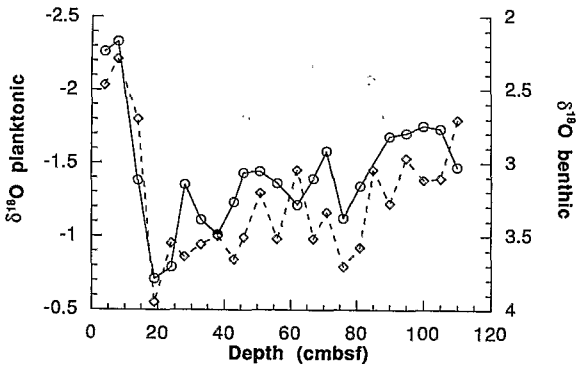

Fig. 4. Plot of $\delta^{18}O$ from planktonic (diamonds) and benthic (circles) foraminifers against depth in core 51GC21.

Table 3. A graphic correlation with the standard benthic reference curve (Martinson et al., 1987) gave an age model for the sequence (Fig. 5). The disappearance of the pink form of *Globigerinoides ruber* at 145 cm bsf marks the transition between Stages 6 and 5 (Thompson et al., 1979), and is consistent with this $\delta^{18}O$ stratigraphy. However, it must be noted that a few discrepancies exist between the planktonic and benthic records. For example, the sample at 24 cm bsf yields a planktonic $\delta^{18}O$ value indicative of Stage 3, but the benthic $\delta^{18}O$ can still be considered to be representing a full glacial value (Fig. 4). Similarly, the Stage 3/5 boundary could be placed between 62 and 67 cm bsf according to the planktonic record, although benthic $\delta^{18}O$ values reach a minimum at 71 cm bsf. Since the planktonic record can be affected by local causes, such as the evaporation/precipitation ratio and sea-surface temperature fluctuations, the benthic record was considered to be a more reliable tool for correlation with standard records. The final Isotope Stage positions were chosen by comparing the 51GC21 benthic record with the stacked benthic records of Pisias et al. (1984) and Labeyrie et al. (1987).

4.2. *Qualitative palaeotemperature estimates*

Twenty samples from core 51GC21 were added to the PCoA ordination (Fig. 6). Overall, Fig. 6 clearly indicates a trend towards cooler waters from sample 1 to sample 20. However, upon detailed examination, a more complex history is revealed, and six intervals can be defined (Fig. 7):

Interval 1: Samples 16–20 (65,000–99,000 yr B.P.); conditions cooler relative to the present-day.

Interval 2: Samples 14–15 (56,000–59,000 yr B.P.); warming trend.

Interval 3: Samples 11–13 (42,000–52,000 yr B.P.); environment similar to the one prevailing today.

Interval 4: Samples 7–10 (29,000–39,000 yr B.P.); cooling trend.

Interval 5: Samples 5–6 (17,000–25,000 yr B.P.); additional cooling. Environmental conditions similar to those of interval 2.

Interval 6: Samples 1–3 (Present–12,000 yr B.P.); present-day environmental conditions prevail for this entire period.

4.3. *Mg/Ca-derived palaeotemperatures*

Bottom-water temperatures (BWT) for core 51GC21 reconstructed from the Mg/Ca record are shown in Fig. 8 (data in Table 3). The present-day water depth at site 51GC21 is 1630 m, and the corresponding water temperature is 2.7°C ± 0.2°C (Corrège, 1993c). This value is similar to that witnessed during the Holocene. During Stage 2 the BWT was significantly lower (approximately 1.1°C). However, high BWT are recorded during part of Stage 3, particularly between 40,000 and 52,000 yr B.P. During this interval, BWT were equal to, or at times even higher by 1°C than, the present-day value. In the lower half of the core, low BWT during Stage 5 (e.g. ranging from 1.6°C to 2.0°C) and higher BWT (e.g. ranging between 2.3°C and 2.8°C) during Stage 5 are recognised, except for a significant cooling change between 90,000 and 100,000 yr B.P. (e.g. temperatures lower than 1.5°C).

4.4. *Reconstructed salinities and densities*

Palaeosalinity and palaeodensity values were calculated following the method described above. The data are presented in Table 4 and in Figs. 9

Table 3
Detail of the chemical analyses for core 51GC21

Depth (cmbsf)	Age (Ky)	δO^{18} plankt. foram.	δO^{18} bent. foram.	Genus	Mg/Ca molar	Temp. (°C)	Mean Temp (°C)
4	1	-2.03	2.24				
8	5	-2.21	2.17	B	0.023018	1.7	2.7
8				B	0.028895	3.8	
14	12	-1.8	3.12				
19	17	-0.55	3.79				
24	21	-0.95	3.71	K	0.0085161	1.1	1.1
24				K	0.0084365	1.1	
28	25	-0.86	3.15	K	0.010723	2.3	2.3
33	29	-0.94	3.39	K	0.0099675	1.9	1.9
38	33	-1,00	3.49				
43	37	-0.84	3.27	K	0.0094298	1.6	1.6
46	39	-0.99	3.07	K	0.010610	2.2	2.7
46				K	0.012577	3.2	
51	42	-1.29	3.06	K	0.011600	2.7	2.8
51				K	0.011922	2.9	
56	47	-0.98	3.14	K	0.011549	2.7	3.1
56				K	0.012779	3.3	
56				K	0.012549	3.2	
62	52	-1.45	3.29	K	0.012271	3.1	3.9
62				K	0.015301	4.7	
62				K	0.013893	3.9	
67	56	-0.98	3.11	K	0.010743	2.3	2.3
71	59	-1.16	2.92	B	0.023565	1.9	1.6
71				K	0.0082852	1.0	
71				K	0.0099879	1.9	
76	65	-0.79	3.38	K	0.010542	2.2	2.0
76				K	0.0095943	1.7	
76				K	0.0087715	1.3	
76				K	0.011398	2.6	
81	73	-0.92	3.16				
85	78	-1.45		K	0.011304	2.6	2.3
85				K	0.014608	4.3	
85				K	0.0082096	0.97	
85				K	0.012144	3.0	
85				K	0.0078919	0.80	
90	91	-1.22	2.82	K	0.0099938	1.9	1.5
90				K	0.0084191	1.1	
95	99	-1.53	2.8	K	0.0085765	1.2	1.2
100	107	-1.38	2.75	K	0.011712	2.8	2.8
105	112	-1.39	2.77				
110	116	-1.79	3.03				

Ages were calculated by graphic correlation with the Martinson et al. (1987) isotopic curve. $\delta^{18}O$ values are given relative to the PDB scale. Code for genus is B = *Bythocypris* and K = *Krithe*. Temperatures were calculated using Eqs. (1) and (2) (see text)

and 10. The present-day salinity at site 51GC21 is 34.6‰ and the temperature is 2.7°C ± 0.2°C (Corrège, 1993c). The corresponding density derived from the graph of Labeyrie et al. (1992) is 27.6, in accordance with values found in the literature (Andrews and Clegg, 1989). The salinity and density reconstructions (Figs. 9 and 10) show three very distinct trends spanning particular periods of time. The only sample available for the Holocene period indicates a salinity and a density similar to the present-day. Before that, there is a long period spanning at least the interval 21,000–65,000 yr B.P. during which salinity and density increased on average by 1.1‰ and 1 unit, respectively. However, a sharp change is present at around 52,000 yr B.P., related to the high BTW

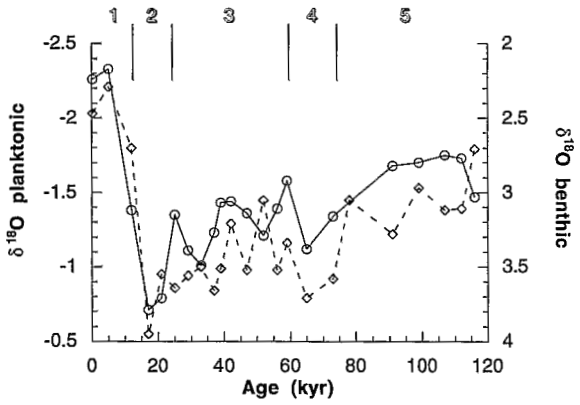

Fig. 5. Plot of $\delta^{18}O$ from planktonic (diamonds) and benthic (circles) foraminifers against time derived from a graphic correlation with the SPECMAP stack of Martinson et al. (1987).

given by the Mg/Ca palaeothermometer. There is also a small trough in both the salinity and density curves at 59,000 yr B.P. Unfortunately, no data are available between 65,000 yr B.P. and 91,000 yr B.P. The third period is situated within Isotope Stage 5, where all three samples have a similar salinity and a density value of 28.1.

The sample at 85 cm bsf has an estimated age of 78,000 yr B.P., just at the transition between Isotope Stages 4 and 5. At that time the reconstructed temperature is 2.5°C but, unfortunately, no benthic foraminifer could be found in this sample and thus no $\delta^{18}O$ data are available. However, considering the rest of the benthic $\delta^{18}O$ record during Stage 5, it seems reasonable to assume a $\delta^{18}O$ value close to $2.9 \pm 0.1‰$. In that

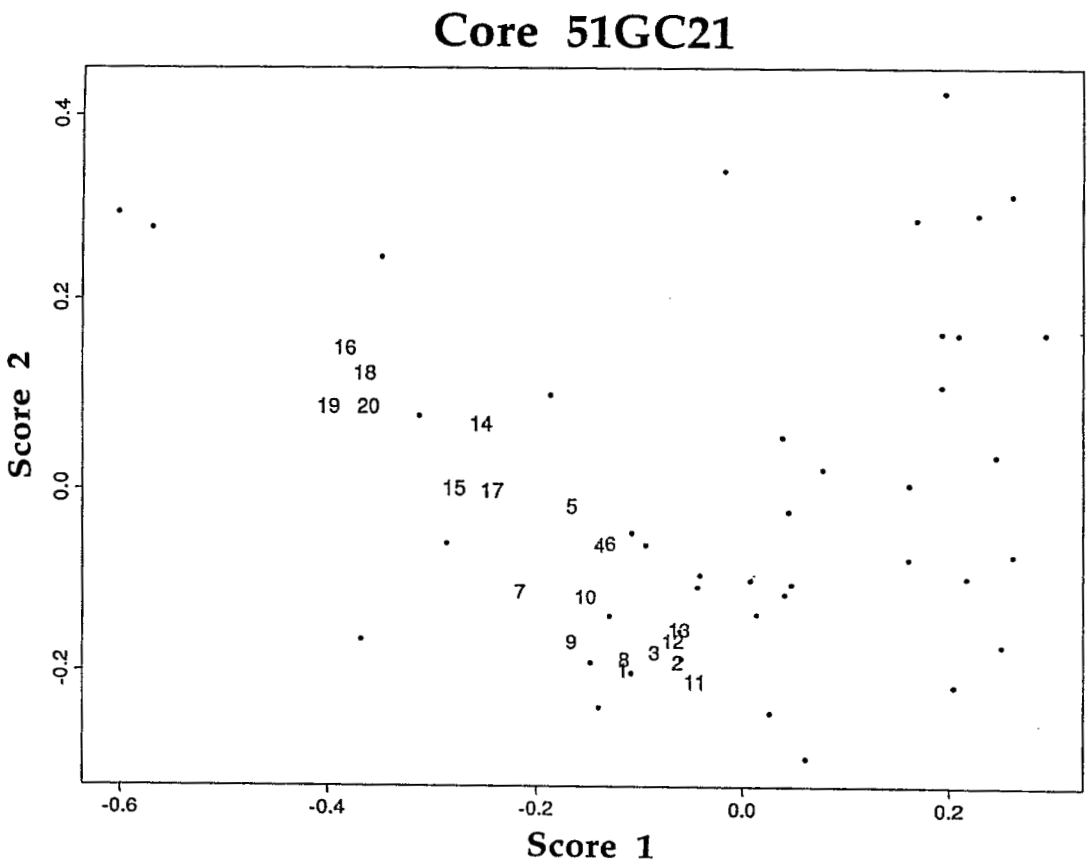

Fig. 6. Plot of Score 1 versus Score 2 for all the samples from core 51GC21, after each sample was added to the PCoA performed on modern surface-sediment samples. The dots represent the modern samples, as they appear in Fig. 2. The numbers refer to core samples (number 1 being the surface-sediment sample, and number 20 the sample taken at 95 cm bsf; see Table 1).

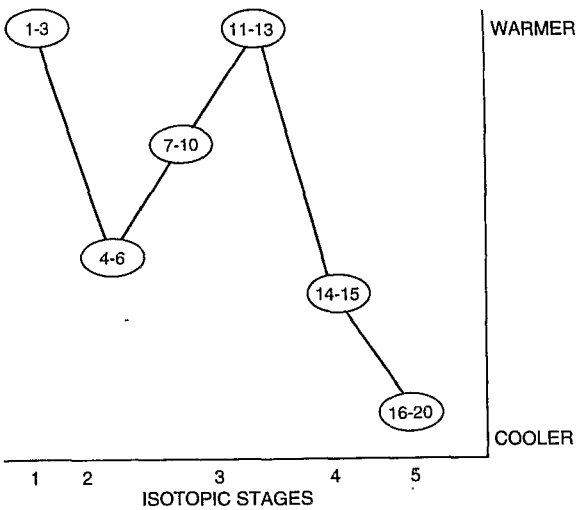

Fig. 7. Sketch to indicate the trend in qualitative water temperature variations through time as revealed by the PCoA presented in Fig. 6. The numbers refer to the core samples described in Fig. 6 and Table 1.

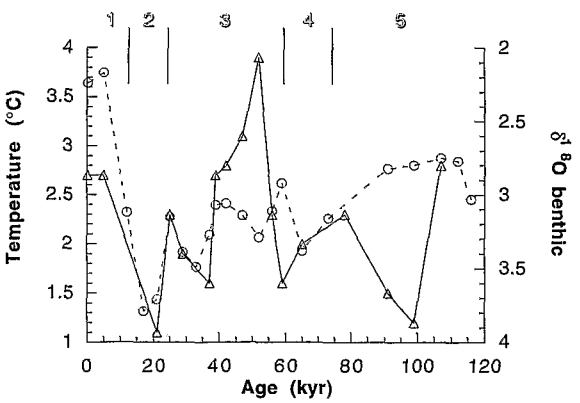

Fig. 8. Record of bottom water temperatures (triangles) and benthic $\delta^{18}O$ record of foraminifers (circles) in core 51GC21 versus age. BWT based on the Mg/Ca of selected ostracods (raw data in Table 3). Shadowed numbers at the top refer to the conventional Isotopic Stages.

case, the salinity at 85 cm bsf would be around 35.5 ± 0.1‰, and the inferred density 28.5 ± 0.1. This value is situated half way between the reconstructed densities for the 65,000 yr B.P. and 91,000 yr B.P. time interval, and is represented by a black square in Fig. 10.

5. Discussion

5.1. Critical assessment of the temperature/salinity/density reconstruction method

5.1.1. Palaeotemperatures

A comparison between Figs. 7 and 8 shows that there is generally good agreement between the qualitative and the quantitative approaches to palaeotemperature estimation. Both methods record the LGM as a low BWT event, and the older portion of Stage 3 as a warm phase with temperatures similar to the present day. However, the PCoA tends to imply that all the BWT between 56,000 yr B.P. and 99,000 yr B.P. (i.e. below 67 cm bsf in the core; samples 14–20) were lower than during the LGM. This result is not substantiated by the data from the Mg/Ca analyses, although some temperatures similar to LGM values are detected at 59,000 yr B.P. (sample 15, 71 cm bsf) and between 91,000 and 99,000 yr B.P. (samples 19 and 20; 90 and 95 cm bsf). The high temperature (i.e. 3.9°C) given by the Mg/Ca analyses at 52,000 yr B.P. (sample 13, 62 cm bsf) is not reflected in the PCoA record.

Despite some differences, these results appear encouraging in the perspective of the development of a palaeotemperature transfer function based on ostracods. The PCoA technique used here was developed from semiquantitative estimates of ostracod populations at the generic level. Although sophisticated statistical analyses can be applied to semiquantitative data sets (Sancetta, 1979), the transfer functions most commonly used in palaeoceanography (i.e. the Imbrie and Kipp (1971) method, and the Modern Analog Technique; Hutson, 1980; Anderson et al., 1989) do require quantitative data sets. Furthermore, it is probable that the identification to species level of some genera which have a wide bathymetric distribution (i.e., *Krithe*, *Cytheropteron*, *Bairdia* and *Argilloecia*, among others; see Corrège, 1993c) could also ameliorate the method.

The Mg/Ca-based palaeotemperature reconstructions could also be improved by several additional means. At present, the method has only been calibrated for a narrow temperature range (i.e. 2–6°C). Any calculated palaeotemperature

Table 4
Detail of the calculations used to obtain bottom water temperatures, salinities and densities for core 51GC21

Depth (cmbsf)	Age (kyr BP)	$\delta^{18}O$ plank.	$\delta^{18}O$ bent.	$\delta^{18}O$ corr.	$\delta^{18}O$ seawater	$\delta^{18}O$ residual	$\Delta_{TS}\delta^{18}O$	$\Delta_{T}\delta^{18}O$	$\Delta_{S}\delta^{18}O$	ΔS (‰)	LSL (m)	ΔS_t (‰)	S_t (‰)	BWT (°C)	Density
4	1	-2.03	2.24	3.07	0.00	3.07	0.00	0.00	0.00	0.00	0	0.00	34.60	2.7	27.6
8	5	-2.21	2.17	3.00	0.05	2.95	-0.12	0.00	-0.12	-0.24	10	0.09	34.45	2.7	27.6
14	12	-1.80	3.12	3.95											
19	17	-0.55	3.79	4.62											
24	21	-0.95	3.71	4.54	1.00	3.54	0.47	0.37	0.10	0.20	114	1.04	35.84	1.1	28.7
28	25	-0.86	3.15	3.98	0.51	3.47	0.40	0.09	0.31	0.62	60	0.54	35.76	2.3	28.6
33	29	-0.94	3.39	4.22	0.65	3.57	0.50	0.18	0.32	0.64	76	0.69	35.93	1.9	28.7
38	33	-1.00	3.49	4.32											
43	37	-0.84	3.27	4.10	0.55	3.55	0.48	0.25	0.23	0.46	65	0.59	35.65	1.6	28.6
46	39	-0.99	3.07	3.90	0.67	3.23	0.16	0.00	0.16	0.32	78	0.71	35.63	2.7	28.5
51	42	-1.29	3.06	3.89	0.58	3.31	0.24	-0.02	0.26	0.52	68	0.62	35.74	2.8	28.6
56	47	-0.98	3.14	3.97	0.57	3.40	0.33	-0.09	0.42	0.84	67	0.61	36.05	3.1	28.7
62	52	-1.45	3.29	4.12	0.45	3.67	0.60	-0.28	0.88	1.76	55	0.50	36.86	3.9	29.2
67	56	-0.98	3.11	3.94	0.58	3.36	0.29	0.09	0.20	0.40	68	0.62	35.62	2.3	28.5
71	59	-1.16	2.92	3.75	0.20	3.55	0.48	0.25	0.23	0.46	27	0.24	35.30	1.6	28.3
76	65	-0.79	3.38	4.21	0.71	3.50	0.43	0.16	0.27	0.54	83	0.75	35.89	2.0	28.7
81	73	-0.92	3.16	3.99											
85	78	-1.45												2.3	
90	91	-1.22	2.82	3.65	0.20	3.45	0.38	0.28	0.10	0.20	26	0.23	35.03	1.5	28.1
95	99	-1.53	2.80	3.63	0.02	3.61	0.54	0.35	0.19	0.38	7	0.06	35.04	1.2	28.1
100	107	-1.38	2.75	3.58	0.51	3.07	0.00	-0.02	0.02	0.04	60	0.54	35.18	2.8	28.1
105	112	-1.39	2.77	3.60											
110	116	-1.79	3.03	3.86											

Ages are interpolated directly from a graphic correlation with the SPECMAP stack of Martinson et al. (1987). All $\delta^{18}O$ data are expressed on the PDB scale. $\delta^{18}O$ corr. is the benthic $\delta^{18}O$ corrected by the fractionation factor for *C. wuellerstorfi* (i.e. 0.83‰; Herguera et al., 1992). $\delta^{18}O$ seawater taken from Labeyrie et al. (1987). For other symbols refer to the text

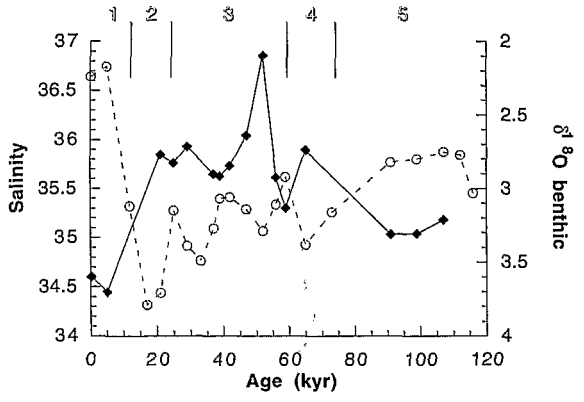

Fig. 9. Reconstructed bottom water salinities (diamonds) and the $\delta^{18}O$ record of benthic foraminifers versus age for core 51GC21. Salinity calculations are presented in Table 2. Isotopic Stages as for Fig. 8.

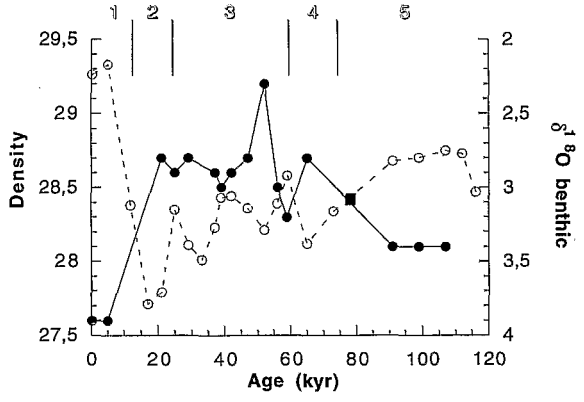

Fig. 10. Reconstructed bottom water densities (dots) and the $\delta^{18}O$ record of benthic foraminifers (circles) versus age for core 51GC21. Density calculations are presented in Table 4. Isotopic Stages as for Fig. 8. The square represents an estimated value assuming a benthic $\delta^{18}O$ value of 2.9 ± 0.1‰. See text for additional information.

below 2°C or above 6°C is therefore highly hypothetical, because we do not know at this stage whether the temperature–Mg/Ca relationship will remain linear for these 'domains'. In fact, to maintain the thermodynamic stability of the ostracod low-magnesium calcitic valves, we anticipate that, both at high and low temperatures, a threshold in the amount of Mg uptake must be reached, implying that the linearity of the relationship is most certainly verified only within a certain 'dynamic' range. As a consequence, there is a need to analyse additional modern ostracod valves which were calcified in waters with temperature below and above the 2–6°C range so as to better constrain the temperature–Mg/Ca relationship. Finally, we observe that the percentage of standard deviation for Mg/Ca measurements in a batch of valves is always lower for fossil material compared to modern samples. This could indicate that our cleaning method for modern valves is rather inadequate and that some organic material may remain attached to the valves, thus allowing some amount of Mg to be accounted for in the analyses, and subsequently increasing the variability in the Mg/Ca measured in a modern ostracod population. This problem requires definite solving because the accuracy of the Mg/Ca palaeothermometer at present is highly dependent upon the percentage of standard deviation of the mean Mg/Ca ratio measured in modern valves (see Fig. 3c).

5.1.2. *Salinity and density*

The potential errors in the reconstructed salinities arise from different sources. First, there is an error on the benthic foraminifer $\delta^{18}O$ measurement (typically ± 0.1‰) which, in salinity terms, represents ± 0.2‰. Then, the variations in seawater $\delta^{18}O$ postulated by Labeyrie et al. (1987) and Duplessy et al. (1988,)) used in the present study can be queried for several reasons: (1) Labeyrie et al. (1987) have suggested that deep-water temperatures have not changed in the Norwegian Sea during the last 130,000 years, but this remains unverified; (2) these authors used a fractionation factor of 0.64‰ for *C. wuellerstorfi* but Herguera et al. (1992) have since shown that a 0.83‰ value could be a better estimate; (3) benthic foraminifers were scarce during the LGM in the Norwegian Sea, and the interpolation attempted by Labeyrie et al. (1987) with the benthic record of V19-30 (from the east Pacific Ocean; Shackleton et al., 1983) yields seawater $\delta^{18}O$ values which are at odds with the findings of Fairbanks (1989).

Another potential source of error arises from the fact that our age model for 51GC21 can be biased because of the low resolution of the isotopic record. Although all the main features identified in 51GC21 could be matched with the SPECMAP stacked record, the precise timing of high and low

$\delta^{18}O$ episodes cannot be determined accurately, particularly for Stage 5. This, of course, has consequences for the values taken from the seawater $\delta^{18}O$ data set of Duplessy et al. (1988,)).

The main source of error in the salinity calculation is, however, associated with the error for the temperature estimate, because the temperature signal is converted into a $\delta^{18}O$ value which we subtract from the residual $\delta^{18}O$. An error of ± 1.5°C in temperature would correspond to an error of 0.35‰ in $\delta^{18}O$ terms, or 0.7‰ in salinity terms.

The choice of the sea-level curve used in the final salinity calculation is also important. Here we use the curve from Labeyrie et al. (1987) so as to be consistent with the seawater $\delta^{18}O$ variations. However, this sea-level curve differs slightly from the one derived from the raised corals of Huon Peninsula (Chappell and Shackleton, 1986). Nevertheless, a recent reappraisal of the Huon Peninsula sea-level curve (Chappell et al., 1994) reflects a better agreement with the data presented here.

Finally, the main difficulty arising from our method is the fact that we compare the Mg/Ca record of ostracod valves with the $\delta^{18}O$ record of benthic foraminifers. These organisms, although found in the same sample, could be of different age due to bioturbation. This problem is particularly important when only one ostracod valve is found in a sample. However, high resolution studies, and the development of the Mg/Ca method on other ostracod genera (thus multiplying the number of valves potentially available for chemical analyses), should eventually help to overcome this deficiency.

In conclusion, it is difficult to assess precisely the error for the reconstructed salinities; at present, we consider that the accuracy is within the ± 0.5–± 1‰ range. For density reconstructions, on the other hand, a ± 1.5°C error on temperature associated with a ± 0.7‰ error for salinity would represent a density error of $\pm 0.6\sigma$.

5.2. *The Late Quaternary TSD history of intermediate water in the Coral Sea*

The temperatures, salinities and densities reconstructed from core 51GC21 provide a window on the oceanographic changes which occurred in the intermediate waters of the western Coral Sea during the last 100,000 years. The results obtained for the Last Glacial Maximum (LGM) (cooling of 1.6°C at 21,000 yr B.P.) are consistent with what was already postulated for this period. In the Pacific, deep-water temperatures were about 2°C cooler during Stage 2 (Chappell and Shackleton, 1986). Surface waters were found to be only slightly cooler in the northern part of the Coral Sea, but up to 3.5°C cooler in the southern part during the LGM (Anderson et al., 1989). In addition to temperature, salinity and density reconstructions clearly show that a different water mass was bathing the site of core 51GC21 during Stage 2. Furthermore, although temperatures returned to values similar to the present-day during part of Stage 3, salinity and density remained relatively stable from 65,000 yr B.P. to 21,000 yr B.P. The only exception is the sample dated at 52,000 yr B.P. The high temperature (i.e. 3.9°C) calculated for this period associated with a slight increase in benthic $\delta^{18}O$ yields a high salinity and density, which do not appear realistic. Three *Krithe* valves were analysed in this sample, two of which were noted as being in a precarious state; the first one had a very narrow inner lamella, and thus could have been a juvenile (see Van Morkoven, 1962, for terminology), while the second one was small (i.e. 650 μm compared to an average of 700–850 μm). Corrège (1993b) noted that, on average, small valves tend to have a higher Mg content. Juveniles or poorly calcified specimens are also known to contain up to 25% of Mg (of the total Mg/Ca), compared to 1–3% normally (Chivas et al., 1983). Therefore, it is probable that the temperature at 52,000 yr B.P. is biased toward a high value when it should essentially be the same as the preceding level (i.e. 3.1°C at 47,000 yr B.P., which is the temperature given by the third ostracod valve at 52,000 yr B.P.).

The observation that salinity, and more importantly density, remained fairly stable between 65,000 yr B.P. and 21,000 yr B.P. has significant consequences for the physical oceanography of the region. If density did not change during this time interval, it implies that the intermediate water circulation pattern, which is driven by density

differences in various parts of the oceans, was also stable during the same period. Similarly, it appears that another stable state was present in the western Coral Sea between 91,000 yr B.P. and 107,000 yr B.P. The resolution is insufficiently high to date the transition between these two periods, but the interpolated density at 78,000 yr B.P. seems to indicate that this change was probably associated with the Stage 4–5 transition.

Today, core 51GC21 is situated in the lower part of the Antarctic Intermediate Water (AAIW). The AAIW forms at the subpolar convergence (i.e. the polar front, 55–60°S) as a low-salinity water mass and travels more than 3,300 km before reaching the Coral Sea. Its salinity increases during this long journey by vertical mixing with the underlying and overlying water masses (Tomczak, 1984). Therefore, at a given location, there is a link between the AAIW salinity and the distance from its source region.

In view of these data, the high salinities and temperatures during part of Stage 3 could be interpreted in various ways:

(1) A longer travel distance could be invoked to account for the high salinity, but it is generally considered that the polar front shifted northward during the last glacial period (CLIMAP, 1976).

(2) A longer travel time for this glacial intermediate water mass, due to a lower velocity, could be an alternative explanation. Shackleton et al. (1988) and Broecker et al. (1988) postulated that, during the LGM, the ventilation rate of deep Pacific water was lower but Duplessy et al. (1988b) found that north of 5°S, intermediate waters (depth range: 700–2,600 m) of the Pacific Ocean had a higher ventilation rate. However, a longer travel time for AAIW could only account for the increase in salinity but not for the high temperatures during Stage 3. In addition, we must emphasise the fact that these results on ventilation rates of the ocean all concern the LGM period, not Isotope Stage 3 events.

(3) Our preferred explanation is that the temperature, and to a lesser extent salinity, of intermediate waters are controlled by the summer insolation in the high latitude of the southern hemisphere (i.e. where these waters sink). A plot of the mean December insolation at 60°S for the last 120,000 years (data from Berger and Loutre, 1991), together with the reconstructed temperatures from core 51GC21 is presented in Fig. 11, bearing in mind that small differences may exist between the oceanic and the astronomic time scales. Between 25,000 yr B.P. and 75,000 yr B.P. there is a striking similarity between the two signals, implying that the temperature of the water mass (as recorded here in the Coral Sea) relates to the summer insolation at 60°S. During Stage 2 the two signals are completely out of phase, confirming the well established climate forcing of the northern hemisphere for this period. During Stage 5 the age model is too incomplete to draw any conclusion, although it seems that, once again, it is the northern, rather than the southern, hemisphere influence which is preponderant.

The peculiar situation during Stage 3 and probably Stage 5 appears to be linked with the low amplitude of insolation variations in the northern hemisphere at that time, compared to the situation in the southern hemisphere (Berger and Loutre, 1991; Fig. 12). During this relatively stable northern hemisphere insolation period the southern hemisphere appears to have played a major role in modulating the oceanography of the Coral Sea. Pichon et al. (1992) noted this southern insolation

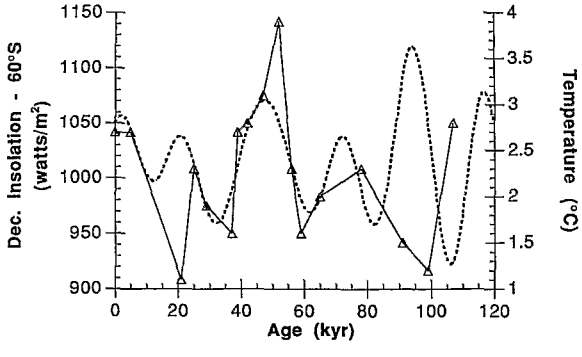

Fig. 11. December (summer) insolation at 60°S (taken from Berger and Loutre, 1991) in stipple and BWT (triangles) versus age. Note the good correlation between the two signals for the period spanning 25,000–65,000 yr B.P.

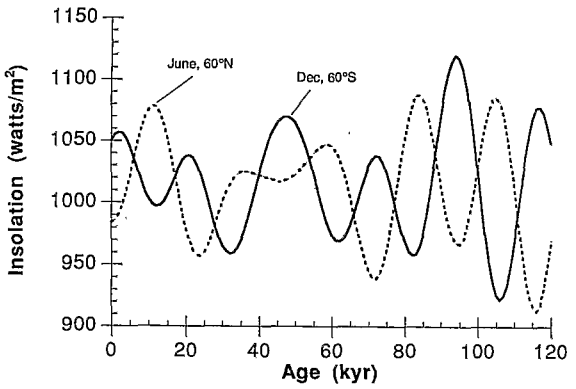

Fig. 12. Summer insolation at 60°N (June) and 60°S (December) for the last 120,000 yr (taken from Berger and Loutre, 1991), showing in particular the small variation in the northern hemisphere for the 30,000 and 65,000 yr B.P. period.

influence on sea-surface temperature in the southern Indian Ocean, although they could not substantiate this phenomenon further. The decoupling between the high northern and the southern latitudes during Stage 3 is not only demonstrated by our data but also by those of Pujol and Turon (1986), who show the influence of northern insolation on climatic indicators in the northern hemisphere.

5.3. *Comparison with the rest of the western Pacific and continental Australia records*

When trying to compare the record from core 51GC21 with other marine records from the western Pacific, or continental records from Australia, we are faced with two problems. For the marine environment, studies are few and tend to concentrate either on the LGM or on a longer time scale (i.e. several million years). In addition, there are even fewer studies which deal with intermediate water masses. On the continent, it is difficult to get a continuous record and, despite some progress with dating techniques, records extending beyond radiocarbon dating are not always reliable. However, for both the marine and continental environments there are some well documented records worthy of comparison with the present results from the Coral Sea.

The Ontong Java Plateau (OJP) is a large submerged plateau located North of the Coral Sea (Fig. 1). It has long been an area of intensive palaeoceanographic studies. However, published benthic $\delta^{18}O$ records from intermediate waters (Herguera et al., 1991, 1992) differ from our own record. In fact, benthic $\delta^{18}O$ records from the OJP seem to indicate that, for both intermediate (Herguera et al., 1991, 1992) and deep waters (Bickert et al., 1993), no cooling occurred during the LGM. Furthermore, carbonate preservation during the Late Quaternary in the Coral Sea (Haddad et al., 1993) and on the OJP (Yasuda et al., 1993) is completely out of phase. Preservation is poor during glacials and good during interglacials in the Coral Sea, and the opposite is true for the OJP. All these results clearly indicate that the two regions have a different palaeoceanographic history, at least for the Late Quaternary. The OJP is probably more influenced by waters forming in a northern source, as proposed by Herguera et al. (1991), whereas the Coral Sea is always under the control of a southern source. This discrepancy between regions situated North and South of New Guinea is further demonstrated by the marine record from the Japan Sea (Oba et al., 1991) which, for the last 85,000 years, has little in common with the Coral Sea record.

Southeast of the Coral Sea, DSDP Site 594 offers a good Quaternary record for comparison with core 51GC21. Site 594 is located about 300 km east of the South Island of New Zealand (Fig. 1), at 1204 m water depth. Detailed benthic $\delta^{18}O$ and percentage of carbonate variations provide the basis for an assessment of oceanographic and climatic change in this region during the last 160,000 years (Nelson et al., 1993). The two main results which can be correlated with the Coral Sea record are: (1) a cooling of 2°C on average during stage 2; and (2) $CaCO_3$ percentages in the lower part of Stage 3 (i.e., 45–55 kyr B.P.) which are almost similar to the percentages recorded during Stages 1 and 5. This latter point suggests that conditions at site 594 between 45 and 55 kyr B.P. were very similar to the present-day one with respect to carbonate deposition and preservation, and therefore could possibly indicate similar temperatures.

As mentioned earlier, well dated records are

rather rare on the continent.&&&&& We will not discuss the LGM period here, but will focus instead on Stage 3. To the best of our knowledge, there is no data on sea-surface temperature in the Coral or Tasman seas during Stage 3, except for a temperature reconstruction based on *Orbulina universa* diameter measurements of De Deckker et al. (work in progress) for a series of cores from the Tasman Sea. The latter work seems to indicate temperatures lower than the present-day at the sea surface in the Tasman Sea during Stage 3, but these results are still preliminary and need to be confirmed. Indeed, if we accept the fact that intermediate waters had temperatures close to the present-day value during part of Stage 3 (Fig. 7), SST for the same period must have been closer to modern values than to LGM values (which were lower by a few degrees. see CLIMAP, 1976 and Anderson et al., 1989). We know that low SST during the LGM are correlated with an extremely dry period in Australia (Bowler and Wasson, 1984). If SST during part of Stage 3 were similar to present day SST, then we would expect a 'wet' phase on the Australian continent (as opposed to the LGMdry phase). Such a wet phase has been identified by various authors during roughly the 40–50 kyr B.P. period (Bowler, 1986; Nanson et al., 1988;Kershaw, 1992). Lakes in southeastern Australia reached their highest level during this period (Bowler, 1986). A distinct pluvial phase was dated between 40 and 50 kyr B.P. by thermoluminescence on a terrace of the Nepean River, near Sydney (Nanson et al., 1988). In Northern Queensland, pollen records from the Atherton Tableland indicate a slightly wetter phase between 40 and 60 kyr B.P. (Kershaw, 1992). All these data suggest high precipitations during part of Stage 3, probably linked to high SST in the Coral and Tasman Seas.

6. Conclusion

The main findings of the present work can be summarised as follows:

(1) Faunal and geochemical evidence suggest that the temperature of intermediate waters in the western Coral Sea has fluctuated drastically during the last 100,000 years.
(2) Mg/Ca ratios measured in benthic ostracod valves have the potential to become a powerful tool for reconstructing past bottom-water temperatures. Coupled with benthic foraminifer $\delta^{18}O$ records, this technique can provide information on past bottom-water salinity and density.
(3) For the last 100,000 years, three distinct oceanographic phases can be recognised from the isotopic salinity and density reconstructions.
(4) Isotope Stage 3 is a period characterised by temperatures similar to the present-day, for the interval 40–55 kyr B.P. for the AAIW. The peculiarity of Stage 3 in the Coral Sea is matched by a continental record from eastern Australia which is characterised by an extremely wet period with apparent sea-surface temperatures lower than for the present.
(5) The Coral Sea record correlates well with that for offshore eastern New Zealand (DSDP Site 594) but is very different from the Ontong Java Plateau. In this context, New Guinea is seen to have acted as an important oceanographic barrier for intermediate water exchange.

Acknowledgements

We thank L. Labeyrie (CFR, Gif sur Yvette) for providing the isotopic data for core 51GC21, Peter Davies (University of Sydney) for access to core 51GC21, collected by the Australian Geological Survey Organisation, and Ross Cunningham (ANU) for help with the statistical analyses. T. Corrège is grateful to D. Burrage for enabling him to participate on 2 R.V. *Franklin* cruises to collect modern ostracod material. Fruitful discussions with John Chappell (ANU) and Jean Jacques Pichon (University of Bordeaux) are also acknowledged. Part of this research was funded by an ANU Ph.D. scholarship awarded to the senior author.

References

Anderson, D.M., Prell, W.L., Barratt, N.J., 1989. Estimates of sea surface temperature in the Coral Sea at the Last Glacial Maximum. Paleoceanography 5, 615–627.

Andrews, J.C., Clegg, S., 1989. Coral Sea circulation and transport deduced from modal information models. Deep-Sea Res. 36, 957–974.

Beiersdorf, H., 1989. Provenance and accumulation rates of Pliocene and Quaternary sediments from the western Coral Sea. Geol. Rundsch. 78, 987–998.

Berger, A., Loutre, M.F., 1991. Insolation value for the climate of the last 10 million of years. Quat. Sci. Rev. 10, 297–317.

Bickert, T., Berger, W.H., Burke, S., Schmidt, H., Wefer, G., 1993. Late Quaternary stable isotope record of benthic foraminifers: Site 805 and 806, Ontong Java Plateau. Proc. ODP, Sci. Results 130, 411–420.

Bowler, J.M., 1986. Quaternary landform evolution. In: Jeans, D.N. (Ed.), Australia — A Geography. Vol. I. The natural environment. Sydney Univ. Press, Sydney, pp. 117–147.

Bowler, J.M., Wasson, R.J., 1984. Glacial age environments of inland Australia. In: Vogel, J.C. (Ed.), Late Cainozoic Palaeoclimates of the Southern Hemisphere. Balkema, Rotterdam, pp. 183–208.

Broecker, W.S., Andree, M., Bonani, G., Wolfli, W., Oeschger, H., Klas, M., Mix, A., Curry, W., 1988. Preliminary estimates for the radiocarbon age of deep water in the glacial ocean. Paleoceanography 3, 659–669.

Burton, E.A., Walter, L.M., 1991. The effect of pCO^2 and temperature on magnesium incorporation in calcite in seawater and $MgCl_2$–$CaCl_2$ solutions. Geochim. Cosmochim. Acta 55, 777–785.

Cadot, H.M., 1974. Magnesium content of calcite in carapaces of benthic marine Ostracoda. Ph.D. Thesis, Univ. Kansas.

Cadot H.M., Kaesler R.L., 1977. Magnesium content of calcite in carapaces of benthic marine ostracods. Pal. Contrib. Univ. Kansas 87, 1–23.

Chappell, J., Shackleton, N.J., 1986. Oxygen isotopes and sea level. Nature 324, 137–140.

Chappell, J., Omura, A., McCulloch, M., Esat, T., Ota, Y., Pandolfi, J., 1994. Revised Late Quaternary sea levels between 70 and 30 ka from coral terraces at Huon Peninsula. In: Ota, Y. (Ed.), Study on Coral Reef Terraces of the Huon Peninsula, Papua New Guinea. A Preliminary Report. Yokohama National Univ., pp. 155–165.

Chave, K.E., 1954. Aspects of the biogeochemistry of magnesium I. Calcareous marine organisms. J. Geol. 62, 266–283.

Chester, R., 1990. Marine Geochemistry. Unwin Hyman, London, 698 pp.

Chivas, A.R., De Deckker, P., Shelley, J.M.G., 1983. Magnesium, strontium and barium partitioning in nonmarine ostracod shells and their use in paleoenvironmental reconstruction — a preliminary study. In: Maddocks, R.F. (Ed.), Applications of Ostracoda. Univ. Houston Geoscience, pp. 238–249.

Chivas, A.R., De Deckker, P., Shelley, J.M.G., 1985. Strontium content of ostracods indicates lacustrine palaeosalinity. Nature 316, 251–253.

Chivas, A.R., De Deckker, P., Shelley, J.M.G., 1986a. Magnesium and strontium in non-marine ostracod shells as indicators of palaeosalinity and palaeotemperature. Hydrobiologia 143, 135–142.

Chivas, A.R., De Deckker, P., Shelley, J.M.G., 1986b. Magnesium content of non-marine ostracod shells: a new palaeosalinometer and palaeothermometer. Palaeogeogr. Palaeoclimatol. Palaeoecol. 54, 43–61.

CLIMAP Project Members, 1976. The surface of the Ice-age Earth. Science 191, 1131–1137.

Corrège, T., 1993a. Preliminary results of paleotemperature reconstruction using the magnesium to calcium ratio of deep-sea ostracode shells from the Late Quaternary of Site 822, Leg 133 (western Coral Sea). Proc. ODP, Sci. Results 133, 175–180.

Corrège, T., 1993b. Late Quaternary palaeoceanography of the Queensland Trough (Western Coral Sea) based on Ostracoda and the chemical composition of their shells. Ph.D. Thesis, Australian National Univ., 213 pp.

Corrège, T., 1993c. The relationship between water masses and benthic ostracod assemblages in the western Coral Sea, southwest Pacific. Palaeogeogr. Palaeoclimatol. Palaeoecol. 105, 245–266.

Cox, R.A., McCartney, M.J., Culkin, F., 1970. The specific gravity/salinity/temperature relationship in natural sea water. Deep-Sea Res. 17, 679–689.

Craig, H., Gordon, L.I., 1965. Deuterium and oxygen 18 variations in the ocean and the marine atmosphere. In: Tongiorgi, E. (Ed.), Stable Isotopes in Oceanographic Studies and Paleotemperatures. CNR, Pisa, pp. 9–130.

Digby, P.G.N., Kempton, R.A., 1987. Multivariate Analysis of Ecological Communities. Chapman and Hall, London, 206 pp.

Duplessy, J.C., Lalou, C., Vinot, A.C., 1970. Differential isotopic fractionation in benthic foraminifera and paleotemperatures reassessed. Science 168, 250–251.

Duplessy, J.C., Labeyrie, L.D., Blanc, P.L., 1988. Norwegian Sea deep water variations over the last climatic cycle: paleoceanographical implications. In: Wanner, H., Siegenthaler, U. (Eds.), Long and Short Term Variability of Climate. Springer, Berlin, pp. 83–116.

Duplessy, J.C., Shackleton N.J., Fairbanks, R.G., Labeyrie, L., Oppo, D., Kallel, N., 1988. Deepwater source variations during the last climatic cycle and their impact on the global deepwater circulation. Paleoceanography 3, 343–360.

Duplessy, J.C., Labeyrie, L.D., Juillet-Leclerc, A., Maitre, F., Duprat, J., Sarnthein, M., 1991. Surface salinity reconstruction of the North Atlantic Ocean during the last glacial maximum. Oceanol. Acta 14, 311–324.

Dwyer, G.S., Cronin, T.M., Baker, P.A., Raymo, M.E., Buzas, J.S., Corrège, T., 1995. North Atlantic deep water temperature change during Late Pliocene and Late Quaternary climatic cycles. Science, submitted.

Fairbanks, R.G., 1989. A 17,000-year glacio-eustatic sea level record: Influence of glacial melting rates on the Younger

Dryas event and deep-ocean circulation. Nature 342, 637–642.

Gower, J.C., 1971. A general coefficient of similarity and some of its properties. Biometrics 27, 857–872.

Haddad, G.A., Droxler, A.W., Kroon, D., Müller, D.W., 1993. Quaternary $CaCO_3$ input and preservation within Antarctic Intermediate Water: Mineralogic and isotopic results from holes 818B and 817A, Townsville Trough (northeastern Australia margin). Proc. ODP, Sci. Results 133, 203–233.

Herguera, J.C., Stott, L.D., Berger, W.H., 1991. Glacial deep-water properties in the west-equatorial Pacific: bathyal thermocline near a depth of 2000 m. Mar. Geol. 100, 201–206.

Herguera, J.C., Jansen, E., Berger, W.H., 1992. Evidence for a bathyal front at 2000 m depth in the glacial Pacific based on a depth transect on Ontong Java Plateau. Paleoceanography 7, 273–288.

Hutson, W.H., 1980. The Aghulas Current during the Late Pleistocene: analysis of modern analogs. Science 207, 64–66.

Imbrie, J., Kipp, N.G., 1971. A new micropaleontological method for quantitative paleoclimatology: application to a Late Pleistocene Caribbean core. In: Turekian, K.K. (Ed.), The Late Cenozoic Glacial Ages. Yale Univ. Press, New Haven, pp. 71–181.

Kershaw, P., 1992. The development of rainforest/savanna boundaries in tropical Australia. In: Furley, P.A., Proctor, J., Ratter, J.A. (Eds.), The Nature of Dynamics of the Forest–Savanna Boundary. Chapman Hall, London, pp. 255–271.

Kitano, Y., Kanamori, N., Oomori, T., 1971. Incorporation of sodium, chloride and sulfate with calcium carbonate. Geochem. J. 5, 183–206.

Labeyrie, L.D., Duplessy, J.C., Blanc, P.L., 1987. Variations in mode of formation and temperature of oceanic deep waters over the past 125,000 years. Nature 327, 477–482.

Labeyrie, L.D., Duplessy, J.C., Duprat, J., Juillet-Leclerc, A., Moyes, J., Michel, E., Kallel, N., Shackleton, N.J., 1992. Changes in the vertical structure of the North Atlantic Ocean between glacial and modern times. Quat. Sci. Rev. 11, 401–413.

Lowenstam, H.A., 1963. Biologic problems relating to the composition and diagenesis of sediments. In: T.W. Donnelly (Ed.), The Earth Sciences: Problems and Progress in Current Research. Univ. Chicago Press, pp. 137–195.

Martinson, D.G., Pisias, N.G., Hays, J.D., Imbrie, J., Moore, T.C., Shackleton, N.J., 1987. Age dating and the orbital theory of the ice ages: development of a high-resolution 0 to 300,000-year chronostratigraphy. Quat. Res. 27, 1–29.

Mucci, A., 1987. Influence of temperature on the composition of magnesian calcite overgrowths precipitated from seawater. Geochim. Cosmochim. Acta 51, 1977–1984.

Nanson, G.C., Price, D.M., Young, R.W., 1988. Thermoluminescence dating of Late Quaternary environmental change in Australia. In: Prescott, J.R. (Ed.), Archaeometry: Australasian Studies 1988. Univ. Adelaide, 71 pp.

Nelson, C.S., Cooke, P.J., Hendy, C.H., Cuthbertson, A.M., 1993. Oceanographic and climatic changes over the past 160,000 years at Deep Sea Drilling Project site 594 off southeastern New Zealand, southwest Pacific Ocean. Paleoceanography 8, 435–458.

Oba, T., Kato, M., Kitazato, H., Koizumi, I., Omura, A., Sakai, T., Takayama, T., 1991. Paleoenvironmental changes in the Japan Sea during the last 85,000 years. Paleoceanography 6, 499–518.

Pichon, J.J., Labeyrie, L., Bareille, G., Labracherie, M., Duprat, J., Jouzel, J., 1992. Surface water temperature changes in the high latitudes of the southern hemisphere over the last glacial–interglacial cycle. Paleoceanography 7, 289–318.

Pisias, N.G., Martinson, D.G., Moore, T.C., Shackleton, N.J., Prell, W., Hays, J.D., Boden, G., 1984. High resolution stratigraphic correlation of benthic oxygen isotopic records spanning the last 300,000 years. Mar. Geol. 56, 119–136.

Pujol, C., Turon, J.L., 1986. Comparaison des cycles climatiques en domaine marin et continental entre 130,000 et 28,000 ans B.P. dans l' hémisphère nord. Bull. Assoc. Fr. l'étude Quat. 25–26, 17–25.

Sancetta, C., 1979. Use of semiquantitative microfossil data for paleoceanography. Geology 7, 88–92.

Savin, S.M., 1977. The history of the earth's surface temperature during the past one hundred million years. Annu. Rev. Earth Planet. Sci. 5, 319–355.

Shackleton, N.J., Imbrie, J., Hall, M.A., 1983. Oxygen and carbon isotope records of east Pacific core V 19-30: implications for the formation of deep water in the Late Pleistocene North Atlantic. Earth Planet. Sci. Lett. 65, 233–244.

Shackleton, N.J., Duplessy, J.C., Arnold, M., Maurice, P., Hall, M.A., Cartlidge, J., 1988. Radiocarbon age of Last Glacial Pacific deep water. Nature 335, 708–711.

Thompson, P.R., Duplessy, J.C., Be, A.H., 1979. Disappearance of pink-pigmented *Globigerinoides ruber* at 120,000 yr BP in the Indian and Pacific oceans. Nature 280, 554–558.

Tomczak, M., 1984. Coral Sea water masses. In: Baker, J.T., et al. (Eds.), Proc. of the Great Barrier Reef Conf., Townsville 1983, pp. 461–466.

Turpen, J.B., Angell, R.W., 1971. Aspects of molting and calcification in the ostracod Heterocypris. Biol. Bull. 140, 331–338.

Van Morkoven, F.P.C.M., 1962. Post Paleozoic Ostracoda. Vol. 1. Elsevier, Amsterdam.

Whitfield, M., 1979. The mean oceanic residence time (MORT) concept, a rationalization. Mar. Chem. 8, 101–123.

Williams, W.T., 1976. Pattern Analysis in Agricultural Science. Elsevier, Amsterdam.

Yasuda, M., Berger, W.H., Wu, G., Burke, S., Schmidt, H., 1993. Foraminifer preservation record for the last million years: Site 805, Ontong Java Plateau. Proc. ODP, Sci. Results 130, 491–508.

Reprinted from

PALAEO
GEOGRAPHY
CLIMATOLOGY
ECOLOGY

Palaeogeography, Palaeoclimatology, Palaeoecology 313 (1997) 183–205

Faunal and geochemical evidence for changes in intermediate water temperature and salinity in the western Coral Sea (northeast Australia) during the Late Quaternary

Thierry Corrège [a,b,*], Patrick De Deckker [b]

[a] *ORSTOM, Laboratoire des Formations Superficielles, 32 Avenue Varagnat, F-93143 Bondy, Cedex, France*
[b] *Department of Geology, Australian National University, Canberra, ACT 0200, Australia*

Received 15 May 1995; accepted 23 August 1996